Rivista Italiana di Paleontologia e Stratigrafia
(*Research in Paleontology and Stratigraphy*)
vol. 131(1): 63-83. **March 2025**
DOI: https://doi.org/10.54103/2039-4942/23510

SHELL MICROSTRUCTURE AND MINERALOGY OF THE MOLLUSC SPECIES *ANADARA UROPIGIMELANA* (BORY DE SAINT-VINCENT, 1827), *TIVELA STEFANINII* (NARDINI, 1933) AND *OLIVA BULBOSA* (RÖDING, 1798)

ANDREA CHIARI, MONICA DAPIAGGI & GAIA CRIPPA*

Università degli Studi di Milano, Dipartimento di Scienze della Terra 'A. Desio', via Mangiagalli 34, Milano, 20133, Italy.
E-mail: andrea.chiari@unimi.it; monica.dapiaggi@unimi.it; gaia.crippa@unimi.it
*Corresponding Author.

Associate Editor: Lucia Angiolini.

To cite this article: Chiari A., Dapiaggi M. & Crippa G. (2025) - Shell microstructure and mineralogy of the mollusc species *Anadara uropigimelana* (Bory de Saint-Vincent, 1827), *Tivela stefaninii* (Nardini, 1933) and *Oliva bulbosa* (Röding, 1798.) *Rivista Italiana di Paleontologia e Stratigrafia*,, 131(1): 63-83.

Keywords: Bivalve; gastropod; biomineral; Scanning Electron Microscopy; X-Ray Diffraction.

Abstract. Mollusc shells are composite structures made of calcite and/or aragonite crystals and biopolymers, arranged in a great variety of microstructures. The formation of shell microstructures is affected by environmental and physiological factors and differences among microstructural types are believed to be of phylogenetic and adaptive biomechanical significance. Here, we characterise and illustrate for the first time, through SEM and XRD analyses, the shell microstructure and mineralogy of specimens of the bivalves *Anadara uropigimelana* (Bory de Saint-Vincent, 1827) and *Tivela stefaninii* (Nardini, 1933), and of the gastropod *Oliva bulbosa* (Röding, 1798), collected in the Upper Holocene HAS1 settlement and in a shell midden in the Khor Rori Archaeological Park (Oman). *Anadara uropigimelana* shows an aragonitic shell with an outer crossed lamellar layer, an inner complex crossed lamellar layer and an irregular simple prismatic pallial myostracum; periodic bands of dendritic nondenticular composite prisms occur in the outer part of the outer layer, reflecting seasonal changes in water temperatures and growth rates. Shells of *Tivela stefaninii* are aragonitic with an outer composite prismatic layer, a middle crossed lamellar layer and an inner complex crossed lamellar layer, whereas those of *Oliva bulbosa* are characterised by an irregular alternation of aragonitic crossed lamellar layers; a transitional layer defined by the occurrence of tidally controlled growth lines, a crossed lamellar callus and a myostracal layer are also described are also described in *Oliva bulbosa*. With this investigation, we provide novel microstructural and mineralogical data on these poorly known mollusc species, providing useful characters for phylogenetic, evolutionary, crystallographic, and palaeoenvironmental studies.

Introduction

Mollusc shells are composite structures build of crystals of calcium carbonate (calcite, aragonite or both) and biopolymers, such as proteins, polysaccharides and lipids, occluded within as well as between the mineral units of the mineralised shell (e.g. Checa & Salas 2017; Griesshaber et al. 2017; Checa 2018). These two classes of materials interlink at all hierarchical levels and create a lightweight product characterised by complex architectures and unique material properties (e.g. Taylor & Layman 1972; Meyers et al. 2008; de Paula & Silveira 2009).

The mineral component shows a great diversity of microstructure and texture patterns combined in different shell layers and has a high potential to be preserved in the fossil record (e.g. Bøggild

Received: May 28, 2024; accepted: October 24, 2024

1930; Kennedy et al. 1969; Kobayashi 1969; Taylor et al. 1969; Taylor 1973; Carter 1990; Checa 2018). This microstructural variety is much more evident in molluscs that in other taxa with calcium carbonate shells or exoskeletons (e.g. Sato & Sasaki 2015). Differences in mollusc shell microstructure are believed to be of phylogenetic and adaptive biomechanical significance. Indeed, microstructural information has been widely used as an important character in phylogenetic analyses and it has long been studied in palaeontology, being a feature that can be inspected in fossil taxa to get inference on evolution and phylogeny of the past life (e.g. Bieler et al. 2014; Sato & Sasaki 2015; Posenato & Crippa 2023). According to Sato et al. (2020) the components of the shell microstructure are generally conservative in evolution, and microstructural differences of shell layers can be useful in discriminating families, genera and even species (Bieler et al. 2014).

The formation of shell microstructures is controlled by physiological and environmental factors (e.g. Carter 1980; Nishida et al. 2011, 2012). Indeed, mollusc shells from different environments (from the intertidal zone to the deep sea) preserve records of environmental and physiological changes in their microstructures, such as changes in crystal size, shape, or mineralogy during their lifetime (e.g. Yamaguchi et al. 2006; Nishida et al. 2012; Schöne & Surge 2012; Posenato et al. 2022). These changes often derive from periodic modifications in the rate of shell deposition associated with variations in chemical composition and crystallographic properties, resulting in a subdivision of the shell into growth increments and growth lines (Schöne & Surge 2012). The discipline analysing these periodic physical and chemical variations in mollusc shells is called sclerochronology (e.g. Jones 1983; Gröcke & Gillikin 2008; Oschmann 2009; Schöne & Gillikin 2013) and provides important information in (palaeo)environmental and (palaeo)climatic studies.

The bivalve species *Anadara uropigimelana* (Bory de Saint-Vincent, 1827) and *Tivela stefaninii* (Nardini, 1933), and the gastropod species *Oliva bulbosa* (Röding, 1798) frequently occur in archaeological shell assemblages of the Arabian region (e.g. Martin 2005; Roselló-Izquierdo et al. 2005; Lindauer et al. 2017, 2018; Callapez & Dinis 2020; Crippa et al. 2024) and are currently living in the Indo-Pacific region (e.g., Tursch & Germain 1985; Lutaenko 2011; Grizzle et al. 2018). Their abundance in archaeological assemblages and the occurrence of clear growth lines and increments in their shells, makes them excellent tools to be used for high resolution palaeoclimatic and palaeoenvironmental studies. However, no data on the shell microstructure of these species have been published, but only scattered information is available on congeneric species (e.g. Kobayashi & Kamiya 1968; Taylor et al. 1969; Kobayashi 1976a, b; Carter 1990; Tursch & Machbaete 1995; Carter et al. 2012; Nishida et al. 2012, 2015; Carter & Sato 2020).

Here, we performed a detailed characterisation, description and illustration of the shell microstructure and mineralogy of specimens belonging to *A. uropigimelana*, *T. stefaninii* and *O. bulbosa* collected in the HAS1 settlement and in a shell midden nearby in the Khor Rori Archaeological Park (Dhofar, Oman), both of Late Holocene (Meghalayan) age. The investigation of shell microstructure and mineralogy through Scanning Electron Microscopy (SEM) and X-Ray Powder Diffraction (XRD), besides being a valuable tool to check fossil shell preservation, is expected to provide novel data on the shell fabric of these poorly known mollusc species, increasing the availability of useful characters for phylogenetic, evolutionary, crystallographic and palaeoenvironmental studies.

Materials and methods

Eleven mollusc specimens belonging to three different species were here analysed: two bivalves, *Anadara uropigimelana* and *Tivela stefaninii*, and one

US	ID number	Species
US30	BS-300 (MPUM 12334)	*Anadara uropigimelana*
	BS-246 (MPUM 12340)	*Tivela stefaninii*
	BS-49 (MPUM 12409)	*Oliva bulbosa*
US54	OS-107 (MPUM 12335)	*Anadara uropigimelana*
	OS-120 (MPUM 12341)	*Tivela stefaninii*
US63	MS-296 (MPUM 12336)	*Anadara uropigimelana*
	MS-24 (MPUM 12411)	*Oliva bulbosa*
US70	A2 (MPUM 12337)	*Anadara uropigimelana*
	T1 (MPUM 12343)	*Tivela stefaninii*
US95	A1 (MPUM 12338)	*Anadara uropigimelana*
	OB1 (MPUM 12413)	*Oliva bulbosa*

Tab. 1 - Species analysed in this study organised by stratigraphic unit (US) with corresponding field ID numbers and repository numbers (MPUM).

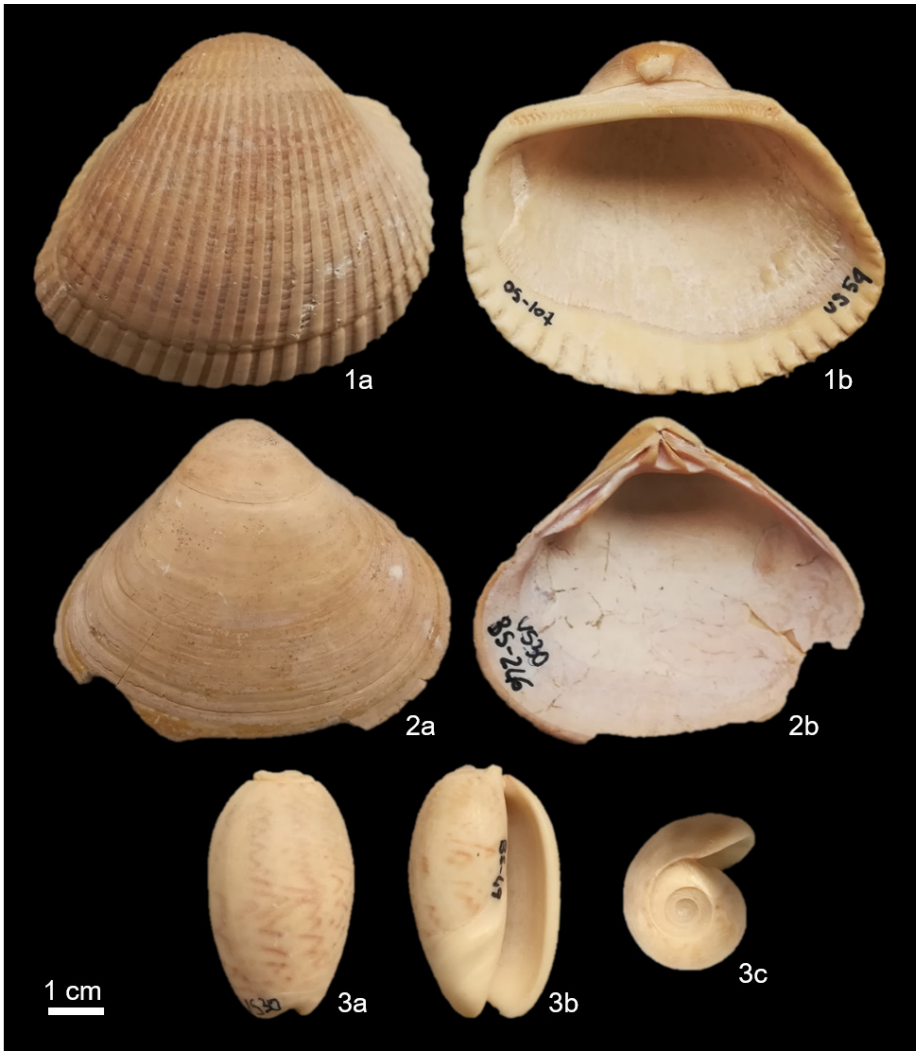

Fig. 1 - Specimens of *Anadara uropigimelana* (1) (OS-107), *Tivela stefaninii* (2) (BS-246) and *Oliva bulbosa* (3) (BS-49) analysed in this study. For bivalves, a: external view, b: internal view. For gastropod, a: abapertural view, b: apertural view, c: apical view.

gastropod, *Oliva bulbosa* (Fig. 1, Tab. 1). All the specimens are currently housed in the collections of the Dipartimento di Scienze della Terra 'A. Desio' of the University of Milan and registered with reference numbers consisting of a prefix MPUM followed by a five-digit number. Reference numbers are given in parentheses after field numbers; the latter are here used for simplicity when referring to the specimens in the text (Tab. 1).

These specimens come from the HAS1 settlement, located on the northern plateau of the Inqitat promontory in the Khor Rori Archaeological Park about 40 km east of Salalah, Dhofar region, southern Oman (17°01'45.2"N, 54°26'32.4"E) (Fig. 2). The settlement is composed of circular or semi-circular megalithic structures formed by a stone basement made by a sandwich wall, filled with soil mixed with rocks of different sizes (Fig. 2 D). The upper part of these structures, probably constituted by perishable material and supported by wooden poles, is not preserved. During the excavation activities traces of the poles and the roof were found carbonised, *in situ* (Lischi 2019, 2023), indicating that the site was engulfed by a fire; this has been also confirmed by a multimethodological study on burned and not-burned mollusc shells from the HAS1 circular structures (Crippa et al. 2023).

The three species here examined were collected from two stratigraphic units within two circular structures (circular structures B5, US30 and B9, US54) and from three stratigraphic units within a shell midden (US63, US70, US95) (Fig. 2 C, D). US indicates a stratigraphic unit. Each US is followed by a number indicating different sampled intervals in the settlement and in the midden.

The stratigraphic unit US30 represents the lowest layer found in the circular structure B5, whereas the stratigraphic unit US54 is found inside the circular structure B9 (Crippa et al. 2024); in both structures carbonised wooden beams and a lot of

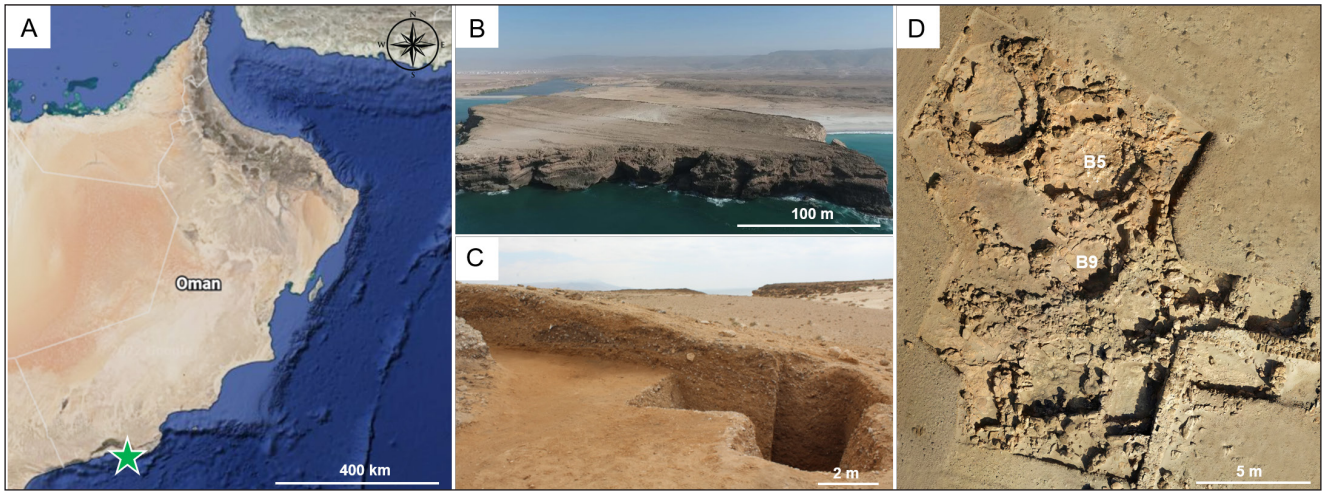

Fig. 2 - Geographical setting: (A) location of the HAS1 settlement in the Dhofar region (green star); (B) northern plateau of the Inqitat promontory where the HAS1 settlement is situated; (C) eastern section of the midden, where specimens from US63, US70, US95 come from; (D) HAS1 settlement showing the position of the circular structures (B5, B9), where specimens from US30 and US54 come from.

fire traces (charcoals) occur, together with some archaeological materials, such as complete potteries.

The other samples were collected in a midden, in the eastern part of the promontory, that has been stratigraphically sampled through an excavated trench nearly 4 meters deep (Fig. 2 C). Three stratigraphic units have been sampled: US63 is the shallower one, followed by US70 and US95 going deeper in the trench. This long stratigraphy stretches from the beginning to the end of the Iron Age (9th century BCE to 2nd century CE).

The HAS1 settlement is dated to the Meghalayan (Late Holocene) and, based on archaeological findings, it was inhabited from at least the 4th century BCE until the 1st-2nd century CE (Middle-Late Iron Age) (Lischi 2018, 2019, 2022, 2023). The stratigraphic units here investigated show the following ages based on radiocarbon dating on animal bones and charcoal (Lischi 2019): US70 (702 – 397 cal BCE), US63 (515 – 349 cal BCE), US30 (385 – 159 cal BCE). US54 and US95 have not been dated, but US54 is coeval with US30, and US95 has an intermediate position between US70 and US98 (843 – 739 cal BCE), and thus an intermediate age.

To characterise the shell microstructure and mineralogy, and check the shell preservation, mollusc specimens were first cleaned from the sediment using a brush to gently remove the soft sediment, then washed with demineralised water and air-dried.

For the microstructural analysis, shell sections were investigated using a JSM-IT500 (JEOL Ltd., Japan) Scanning Electron Microscope (SEM) at the Dipartimento di Scienze della Terra "A. Desio" of the University of Milan, Italy. For sample preparation, we followed the procedure proposed by Crippa et al. (2016) for fossil brachiopod shells. Bivalve specimens were cut in half longitudinally along the axis of maximum growth using a low speed saw with a thin diamond blade, whereas gastropod specimens were cut transversely. One half of each shell was cut again in order to obtain a slice about 1 cm-thick; the remaining part of each half valve/specimen was crushed to a fine powder using an agate mortar and pestle and analysed by X-ray Powder Diffraction (XRD) using a Panalytical X'pert Powder Diffractometer (Panalytical B.V., Netherlands) at the Dipartimento di Scienze della Terra of the University of Milan, Italy.

Each 1 cm-thick slice was glued on glass slides using a two-component epoxy resin, ground smooth using silicon carbide (SiC) powder of two different granulometries and etched with 5% hydrochloric acid (HCl) for 10 seconds to reveal the detail of the microstructure. After washing with demineralised water and drying, each section was coated with gold and observed using the SEM.

SEM images were taken using a secondary electron detector (SED), which provide high-resolution topographical information of the analysed sample surface. However, in some specimens (BS-246, OS-120, T1 and A1), the fracturing occurring during the specimen preparation did not allow to obtain clear and defined images of the shell microstructure

with SED; to overcome this problem, images were also obtained with a backscattered electron detector (BED-C). Photos taken with BED-C are generally worse than SED images in terms of topographical and morphological information obtained, but their quality is enough to characterise the different elements of the shell microstructure in particular situations when clear photos with secondary electrons cannot be acquired.

To define the mineralogical composition and to verify that the specimens are pristine, powdered shells were analysed by XRD. Based on the available literature on these species or other congeneric species, all the examined mollusc shells are aragonitic (Kobayashi & Kamiya 1968; Taylor et al. 1969; Kobayashi 1976 a, b; Carter 1990; Tursch & Machbaete 1995; Carter & Sato 2020); aragonite is a metastable form of calcium carbonate that is commonly replaced by calcite during diagenesis (e.g. Milano et al. 2016; Casella et al. 2017).

The powders (~0,5 g and mean size = ~50–60 μm) were inserted in a back-mounting sample holder to reduce preferential orientation. The X-ray tube (Cu Kα wavelength) was set at 40 kV and 40 mA, and data were collected between 5° and 90° 2θ, with a step size of about 0.02° 2θ and a counting time per step of 30 seconds. The incident slit was fixed at 1/2°, with an antiscatter of 1/2°; the detector used was a multistrip X'Celerator.

Results

Shell preservation

The investigation of mollusc shells at the XRD allows us to characterise their mineralogical phase and to differentiate between aragonite and calcite. XRD analyses indicate that the three mollusc species studied in this work (*Anadara uropigimelana, Tivela stefaninii* and *Oliva bulbosa*) have an aragonitic shell. The diffractogram of each specimen was compared with the characteristic spectra of calcite and aragonite, confirming aragonite as the major mineral component of the shell and the absence of a calcitic phase which would have indicated shell alteration (Fig. 3). The excellent preservation of the specimens is also supported by SEM analysis (see next paragraph) where no sign of diagenetic or anthropic alteration (e.g. sparry calcite) was observed in the aragonitic microstructures.

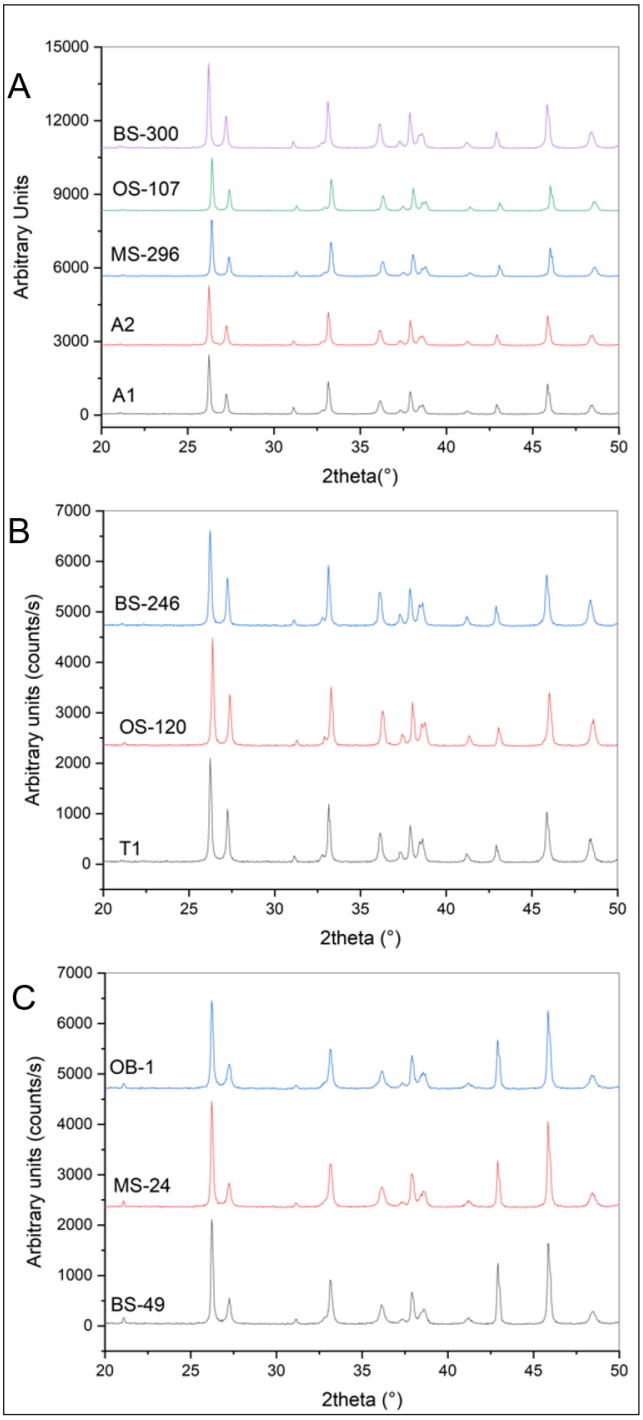

Fig. 3 - Diffractograms for specimens of *Anadara uropigimelana* (A), *Tivela stefaninii* (B) and *Oliva bulbosa* (C) labelled with specimen field numbers. The main peaks indicate that all the shells are composed of aragonite.

Shell microstructure

We follow Carter & Sato (2020) for the terminology used in the microstructural descriptions and to define shell layers (outer, middle and inner). Concerning *Oliva bulbosa*, we prefer to use the terms outer, middle, and inner layers instead of the Mac-

Clintock's (1967) numerical system, which is mainly used for Patellogastropoda and is based on the occurrence of a myostracum separating inner and middle/outer layers, a character not occurring in *O. bulbosa*. Also, as noted by Carter & Sato (2020), the MacClintock's (1967) numerical system typically results in unlikely homologies among layers.

Anadara uropigimelana - Specimens of *Anadara uropigimelana* show an aragonitic shell (Fig. 3 A) with an outer crossed lamellar (CL) layer, an inner complex crossed lamellar (CCL) layer and an irregular simple prismatic pallial myostracum; furthermore, periodic bands of dendritic nondenticular composite prisms (dendritic NDCP) occur in the outer part of the outer layer (Pls 1, 2; Pl. S1 in the Supplementary Material).

Outer layer. The outer layer occupies the outer part of the shell, from the hinge to the ventral margin; its thickness is not constant through the section: it shows its maximum thickness in the hinge plate and in the ventral margin, whereas its minimum occurs dorsally at the umbonal curvature. It is composed of simple crossed lamellae that change from branching crossed lamellae in the outer part of the layer to linear crossed lamellae in the middle and inner part, toward the contact with the inner layer (Pl. 1, figs 1, 5-8; Pl. S1, figs 5, 6 in the Supplementary Material). The degree of the branching changes in the different specimens and is particularly developed in specimens OS-107 and MS-296 (Pl. 1, figs 7, 8). First order lamellae are clearly observable at the SEM by the alternated brightness of the adjacent first order lamellae, which are tilted in two opposite directions (Pl. 1, figs 1, 5, 6; Pl. 2, figs 1-4); they have a variable thickness, generally ranging between 5 and 25 μm.

Inner layer. The inner layer is separated from the outer layer by the pallial myostracum (Pl. 2, figs 1-4). This layer is present only internally with respect to the pallial line and is absent in the hinge plate. The microstructure of the inner layer is mainly composed of irregular complex crossed lamellae with irregularly shaped, laterally interdigitating first order lamellae (Pl. 2, figs 1-6). Rarely, first order lamellae seem to be arranged cone in cone, resembling cone complex crossed lamellae (Pl. 2, fig. 7).

Pallial myostracum. The outer and the inner layers are sharply separated by a pallial myostracum, which is clearly observable in specimens A1 and A2 (Pl. 2, figs 1, 2). It starts at the pallial line and finishes abruptly at the internal margin of the hinge plate. It is composed of simple irregular prism of aragonite and has a thickness of ca. 5 μm (Pl. 2, figs 1, 2). In the specimens where the pallial myostracum is lacking (OS-107 and MS-296), the boundary between outer and inner layers is sharp and defined by a groove (Pl. 2, figs 3, 4). In the umbonal zone of specimen OS-107, the simple irregular prismatic pallial myostracum does not coincide with a change in microstructure between outer and inner layers (Pl. S1, fig. 8 in the Supplementary Material).

Other layers. In three specimens (BS-300, MS-296 and A2) an additional layer is observed in the outer layer, which is lacking or, more likely, not preserved in the other two specimens (A1 and OS-107). The microstructure of this layer is dendritic nondenticular composite prismatic and it is characterised by second order prism diverging from a central, longitudinal core toward the side of the first order prism (Pl. 1, figs 2-5; Pl. S1, fig. 4 in the Supplementary Material). This layer is not continuous along the longitudinal section of the shell, but is locally present in nearly periodic bands (50-150 μm-thick) in the outer part of the outer layer, interrupted and separated by major growth lines (Pl. 1, fig. 5). The transition between these bands and simple crossed lamellae of the outer layer is gradual (Pl. 1, figs 2, 4, 5; Pl. S1, figs 1-3 in the Supplementary Material).

Plate 1

Scanning Electron Microscope images showing the shell microstructure of specimens of *Anadara uropigimelana*. CP: dendritic nondenticular composite prismatic layer; GL: growth lines; IL: inner layer; OL: outer layer; OS: outer surface.

Fig. 1 - Sharp boundary between outer and inner layers near the ventral margin; in the outer layer crossed lamellae pass gradually from linear to branching towards the external shell surface. Specimen A1, right valve.

Figs 2-4 - Dendritic nondenticular composite prismatic microstructure. Second order prisms diverge from a central, longitudinal core toward the side of first order prisms. Specimen BS-300, fragment (2, 3), specimen MS-296, left valve (4).

Fig. 5 - Dendritic nondenticular composite prismatic band near the outer shell surface. The growth line crosses only the linear crossed lamellar outer layer. Specimen MS-296, left valve.

Fig. 6 - Well-preserved crossed lamellar microstructure in the outer layer. First, second and third order lamellae are clearly observable. Specimen BS-300.

Figs 7-8 - Branching crossed lamellae in the outer layer. Specimen MS-296, left valve.

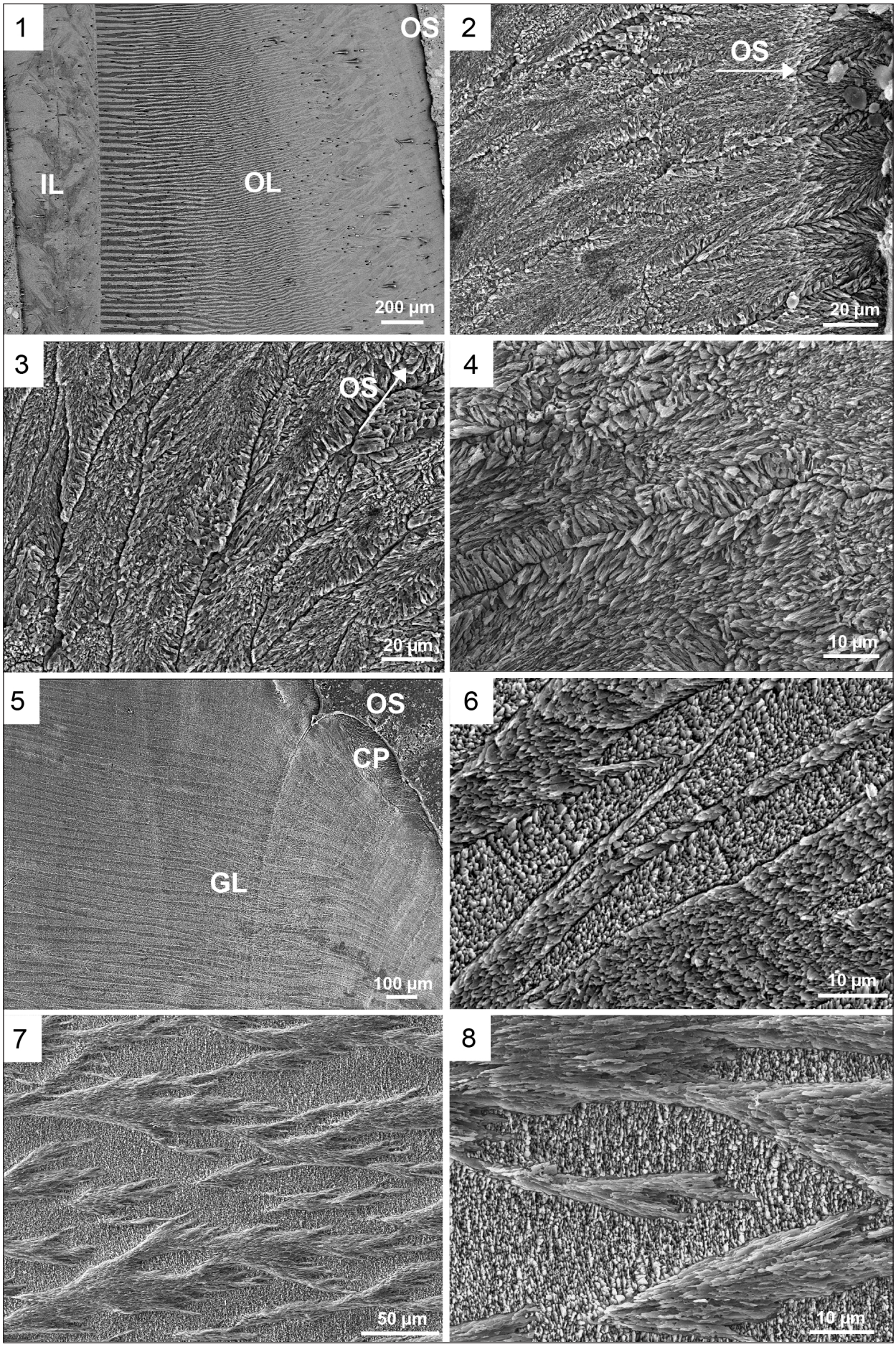
1
OS
IL
OL
200 µm
2
OS
20 µm
3
OS
20 µm
4
10 µm
5
OS
CP
GL
100 µm
6
10 µm
7
50 µm
8
10 µm

Plate 1

Growth lines. Major and minor growth lines are visible along all section (Pl. 1, fig. 5). Their microstructure is generally well-defined and it is composed of irregular simple prisms (Pl. 2, figs 2, 5; Pl. S1, fig. 5 in the Supplementary Material); sometimes prisms are less defined and growth lines correspond to bands with a higher porosity (Pl. 2, fig. 7; Pl. S1, fig. 7 in the Supplementary Material). Growth lines cross both outer and inner layers, but with a different orientation. In the outer layer growth lines are inclined with respect to the shell surface, then curving and becoming nearly parallel to the shell surface and the pallial myostracum toward the inner part of the outer layer; in the inner layer they are parallel to the shell surface and to the pallial myostracum. In the outer layer major growth lines cross only the crossed lamellar microstructure (Pl. 1, fig. 5; Pl. S1, fig. 5 in the Supplementary Material), and not the dendritic NDCP one. In the examined specimens, major growth lines are characterised by the formation of steps on the outer shell surface (Pl. 1, fig. 5).

Tubules. The shell of specimens of *Anadara uropigimelana* is crossed by tubules. Tubules perforate all the shell layers, from the inner to the outer layers. However, their appearance is restricted to the part of the shell inside the pallial line, that is characterised by the inner layer (Pl. 1, fig. 1, Pl. 2, figs 1, 2, 4, 6-8). No tubule has been found starting outside the pallial line, in the marginal band or in the hinge plate. They appear as empty perforations, 3-10 μm in diameter, crossing continuously both the outer and inner shell layers and perpendicular to external shell surfaces (Pl. 1, fig. 1, Pl. 2, figs 1, 2, 4; Pl. S1, figs 6, 8 in the Supplementary Material). The number of perforations varies among the specimens: the shell of OS-107 is continuously and regularly perforated from the ventral margin to the dorsal region, whereas in A2 the presence of tubules is irregular along the section.

Tivela stefaninii - Specimens of *Tivela stefaninii* show an aragonitic shell (Fig. 3 B) with an outer composite prismatic layer, a middle crossed lamellar layer and an inner complex crossed lamellar layer (Pls 3, 4; Pl. S2 in the Supplementary Material).

Outer layer. The outer layer is not continuous along the section and frequently alternates with the middle layer on the outer shell surface. This discontinuous occurrence may be due to shell preparation and its peculiar fragility, or because of the specimen preservation. The outer layer is composed of first order prisms formed by second order fibrous prisms radiating from a spindle, toward the depositional surface (Pl. 3, figs 1-5; Pl. S2, figs 1, 2 in the Supplementary Material); the apex of fibrous prisms is often etched more quickly compared to the surrounding parts, resulting in the black holes observed in the images (Pl. 3, figs 1-4); each second order fibrous prisms seem to be composed of lower order thin prisms radiating in a fan-like way from a central longitudinal axis (Pl. 3, figs 2, 3, 6). This microstructure is a composite prismatic seemingly with a spherulitic origin. The transition from the outer to the middle layer is gradual (Pl. 3, fig. 7).

Middle layer. The middle layer is characterised by a simple crossed lamellar microstructure, with linear first order lamellae (Pl. 3, figs 7, 8, Pl. 4, figs 1, 2; Pl. S2, figs 3-6 in the Supplementary Material). The thickness of first order lamellae is constant, ranging between 5 and 15 μm. The etching highlighted a lower order structure of the lamellae; they seem to be composed of thin prisms radiating in a fan-like way from a central longitudinal axis, as observed in the second order prisms of the composite structure of the outer layer (Pl. S2, fig. 3 in the Supplementary Material).

Inner layer. The inner layer is composed of a distinct fine complex crossed lamellar microstructure, characterised by isolated and elongated structural units not arranged into first order or second

---

Plate 2

Scanning Electron Microscope images showing the shell microstructure of specimens of *Anadara uropigimelana*. GL: growth lines; IL: inner layer; PM: pallial myostracum; OL: outer layer.

Figs 1-2 - Inner and outer layers separated by an irregular simple prismatic pallial myostracum. Tubules cross all layers. Specimen A2, right valve.

Figs 3-4 - Boundary between inner and outer layers not defined by a pallial myostracum, but only by a sharp change in microstructure: linear crossed lamellae in the outer layer and irregular complex crossed lamellae in the inner layer. Tubules cross all layers (4). Specimen OS-107, left valve.

Fig. 5 - Irregular simple prismatic microstructure of a major growth line in the outer layer. Specimen OS-107, left valve.

Fig. 6 - Irregular complex crossed lamellar inner layer crossed by tubules. Specimen MS-296, left valve.

Fig. 7 - Irregular complex crossed lamellar inner layer crossed by tubules and growth lines. In the latter, the irregular simple prisms are less defined and the growth line correspond to a band with a higher porosity. Specimen OS-107, left valve.

Fig. 8 - Detail of a tubule crossing the irregular simple prismatic microstructure of a growth line in the inner layer. Specimen OS-107, left valve.

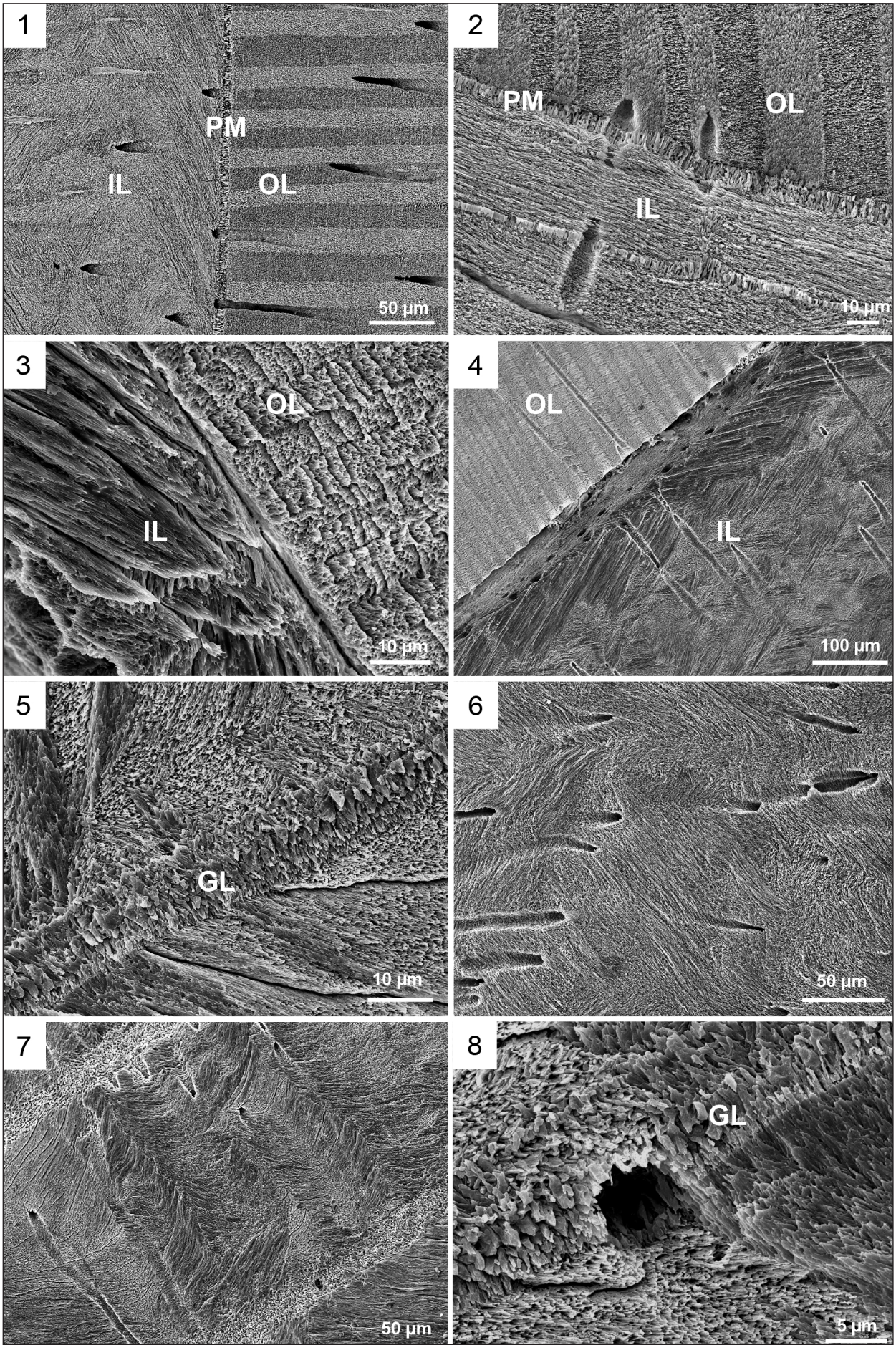
1
PM
IL
OL
50 µm
2
PM
OL
IL
10 µm
3
OL
IL
10 µm
4
OL
IL
100 µm
5
GL
10 µm
6
50 µm
7
50 µm
8
GL
5 µm

PLATE 2

order lamellae (Pl. 4, figs 2-6; Pl. S2, figs 7, 8 in the Supplementary Material). It starts near the ventral margin, occurring only internally with respect to the pallial line.

Pallial myostracum. In the analysed specimens the boundary between middle and inner layers is not defined by a pallial myostracum. Indeed, simple crossed lamellae of the middle layer pass gradually into the fine complex crossed lamellae of the inner layer (Pl. 4, fig. 2).

Growth lines. Major and minor growth lines are observable in all layers (Pl. 3, fig. 7, Pl. 4, figs 1, 2, 4-6; Pl. S2, figs 1-5, 7, 8 in the Supplementary Material). Their microstructure is generally composed of irregular simple prisms (Pl. 4, figs 1, 2, 4-6; Pl. S2, figs 1, 3, 7, 8 in the Supplementary Material). However, this microstructure is not always clear and visible; indeed, in some cases, growth lines are visible due to their different brightness with respect to the surrounding layer. Looking in more detail these growth lines consist of an increase in size and in a change in shape of the basic structural units, forming an aligned line of small prisms; this often coincides also with the occurrence of a thin line with a higher porosity (Pl. 4, figs 1, 2; Pl. S2, figs 2, 4, 5 in the Supplementary Material). In the outer layer growth lines are inclined with respect to the shell surface, then curving and becoming nearly parallel to the shell surface toward the inner part of the outer layer; in the inner layer they are parallel to the shell surface. All the examined specimens are characterised by numerous growth lines (Pl. S2, figs 1-5, 7, 8 in the Supplementary Material).

Oliva bulbosa - Specimens of *Oliva bulbosa* have an aragonitic shell (Fig. 3 C) characterised by an alternation of several layers with a crossed lamellar microstructure (Pls 5, 6; Pls S3-S5 in the Supplementary Material).

Outer layer. The outer layer is composed of linear and slightly branching crossed lamellae (Pl. 5 figs 1, 2; Pl. S3, Pl. S4, fig. 5, Pl. S5, fig. 3 in the Supplementary Material). This layer is continuous along the shell section, decreasing in thickness and closing towards the columella. First order lamellae show different orientations with respect to the outer shell surface, from oblique to parallel in transversal section (Pl. 5, figs 1, 2; Pl. S3, figs 1, 4 in the Supplementary Material) to perpendicular in longitudinal section (Pl. S3, fig. 2). In one specimen (MS-24) in the portions near the columella, crossed lamellae become more complex, with third order lamellae dipping in at least three different directions (Pl. S5, fig. 4 in the Supplementary Material). The outer layer is generally separated from the middle layer by a sharp limit, where branching crossed lamellae of the outer layer pass to linear crossed lamellae of middle layer (Pl. S3, figs 4, 5 in the Supplementary Material). This limit, however, occurs only in limited parts of the shell due to the occurrence of a transitional layer between outer and middle layers (Pl. 5, figs 3-6; Pl. S3, figs 2, 4, 5, 8 in the Supplementary Material).

Transitional layer. Between the outer layer and the middle layer a transitional layer has been observed. This layer is characterised by the occurrence of numerous growth lines (Pl. 5, figs 3-6; Pl. S3, figs 2, 4, 5, 8, Pl. S4, figs 1-5 in the Supplementary Material). In some parts of the shell this layer shows the branching crossed lamellar microstructure of the outer layer, but crossed by numerous growth lines (Pl. 5, fig. 5; Pl. S4, figs 1, 2 in the Supplementary Material); in other parts of the shell the microstructure is not well defined because it is entirely masked by the irregular prismatic microstructure of the growth lines (Pl. 5, figs 3, 6; Pl. S3, fig. 8, Pl. S4, figs 3, 4 in the Supplementary Material). This layer is generally continuous along the section; when not continuous, it occurs in patches characterised by sets of growth lines (Pl. 5, fig. 4; Pl. S4, fig. 5 in the Supplementary Material).

PLATE 3

Scanning Electron Microscope images showing the shell microstructure of specimens of *Tivela stefaninii*. GL: growth lines; ML: middle layer; OL: outer layer.

Figs 1-6 - Composite prismatic microstructure of the outer layer. First order prisms are formed by second order fibrous prisms radiating from a spindle, toward the depositional surface; the apex of fibrous prisms is often etched more quickly compared to the surrounding parts, resulting in the black holes observed in the images (1-4). Each second order fibrous prisms seem to be composed of lower order thin prisms radiating in a fan-like way from a central longitudinal axis (2, 3, 6) Specimen T1, left valve (fig. 1 image in BED-C, 3), specimens OS-120, right valve (2, 6), specimen BS-246, right valve (4, 5).

Fig. 7 - Growth lines crossing the composite prismatic outer layer and crossed lamellar middle layer. The transition between the two layers is gradual. Specimen OS-120, right valve.

Fig. 8 - Linear crossed lamellae in the middle layer. Specimen T1, left valve, image in BED-C.

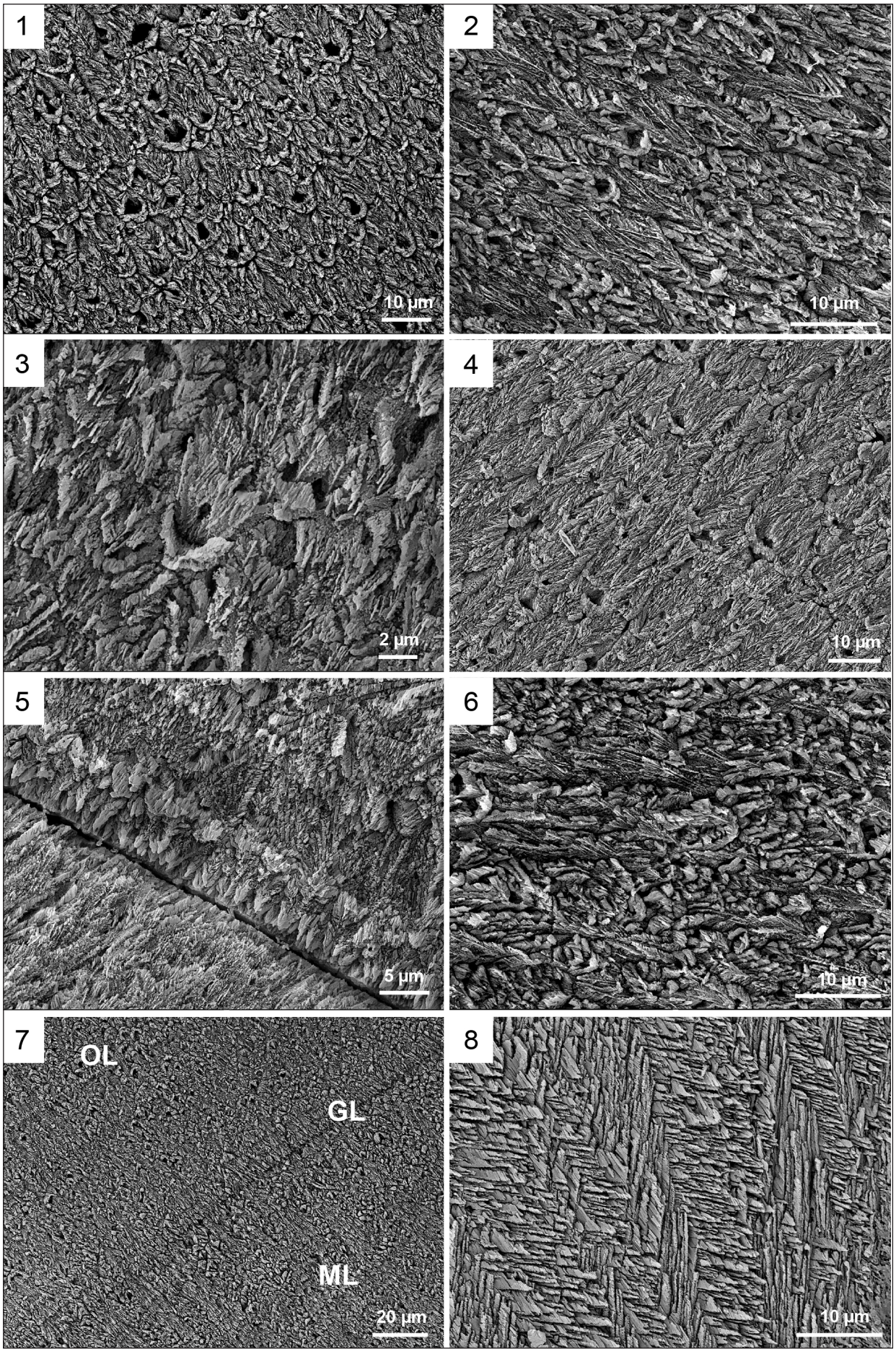

PLATE 3

Middle layer. Between the transitional layer and the inner layer a middle layer is present. This layer is composed of two sublayers showing a different orientation of the crossed lamellae. We here refer to these sublayers as middle layer 1 and middle layer 2. The middle layer 1 is composed of a linear crossed lamellar microstructure (Pl. 5, fig. 8, Pl. 6, figs 1, 2; Pl. S3, figs 1, 2, 4, 5, 8, Pl. S4, figs 5, 6 in the Supplementary Material). This layer occurs along the entire shell section between the transitional layer or, when this is not present, the outer layer, and the middle layer 2. It has a constant thickness along the shell section and decreases towards the columella. First order lamellae are straight, perpendicular to the shell external surface, having a thickness of about 20-30 μm. The boundary with the middle layer 2 is sharp and characterised by a marked change in the orientation of the linear crossed lamellae (Pl. 5, fig. 8; Pl. 6, figs 1, 2; Pl. S4, fig. 6 in the Supplementary Material). The middle layer 2 is composed of linear crossed lamellae (Pl. 5, figs 1, 8, Pl. 6, figs 1-5; Pl. S3, figs 1, 2, Pl. S4, fig. 6 in the Supplementary Material). This layer has a variable thickness along the shell, but it generally increases in thickness near the columella. First order lamellae in the linear crossed lamellar microstructure are oriented obliquely with respect to the outer shell surface in transversal section (Pl. 6, fig. 1; Pl. S4, fig. 1 in the Supplementary Material) and perpendicularly in longitudinal section (Pl. S4, fig. 2 in the Supplementary Material).

Inner layer. The inner layer occurs in the innermost part of the shell and is constituted by a linear crossed lamellar microstructure (Pl. 6, figs 2-5; Pl. S5, fig. 2 in the Supplementary Material). Linear crossed lamellae are generally oriented perpendicularly to the outer surface. The inner layer has a variable thickness along the shell section, increasing towards the columella. In the analysed specimens the boundary between the middle layer 2 and the inner layer is defined by a thin continuous layer with an irregular simple prismatic microstructure (Pl. 6, figs 3-5; Pl. S5, figs 1, 2 in the Supplementary Material).

Other layers. SEM analyses allow to identify and describe other two layers in *Oliva bulbosa* shells. The first occurs in the outer part of the inner whorls as an additional layer outside the outer layer. It is characterised by a linear crossed lamellar microstructure with first order lamellae oriented perpendicularly to the outer shell surface, as in the middle layer 1, being separated from the outer layer by a stockade of irregular simple prisms (Pl. S3, fig. 3 in the Supplementary Material). It has a variable thickness, with its minimum at its appearance in the inner whorls, reaching up to 200 μm (in specimen BS-49), and subsequently decreasing and closing towards the columella.

Also, only in specimen MS-24, near the columella, a further external layer is observed, consisting in a stockade of irregular simple prismatic prisms (Pl. 6, fig. 6; Pl. S5, figs 3, 4 in the Supplementary Material); this layer is preserved in the outer part of the columella.

Growth lines. Growth lines are clearly observable throughout the shell section. In the outer, middle 1 and middle 2 layers the growth lines are curved, following the outline of the aperture (Pl. 5, figs 2-7; Pl. S3, figs 4-8, Pl. S4, figs 1-4 in the Supplementary Material), while in the inner layer they are parallel to the external and internal shell surfaces (Pl. 6, fig. 3; Pl. S5, figs 1, 2 in the Supplementary Material). Major growth lines show a microstructure composed of a stockade of irregular simple prisms and cross the outer and middle layers (Pl. 5, figs 2, 7; Pl. S3, figs 4, 6, 7, Pl. S5, figs 1, 2 in the Supplementary Material). In the transitional layer numerous minor growth lines occur, not extending in the outer and middle layers (Pl. 5, figs 3-6; Pl. S3, figs 1, 2, 5, 8, Pl. S4, figs 1-5 in the Supplementary Material). The microstructure of minor growth lines is not always clear; they are often visible due to their different brightness with respect to the surrounding layer and they are frequently highlighted by the occurrence of a thin line with a higher porosity.

Discussion

Anadara uropigimelana

Specimens of *Anadara uropigimelana* have an aragonitic shell characterised by an outer and inner crossed lamellar layer, separated by a pallial myostracum, and by dendritic NDCP periodic bands in the outer part of the outer layer. All the shell is crossed by growth lines and tubules.

Previous studies analysed the microstructure of modern and fossil specimens belonging to different species of *Anadara*, namely *A. antiquata* (Linnaeus, 1758), *A. obesa* (G. B. Sowerby I, 1833), *A. amicula* (Yokohama, 1925), *A. ninohensis* (Otuka, 1934) and *A. notabilis* (Röding, 1798) (Kobayashi &

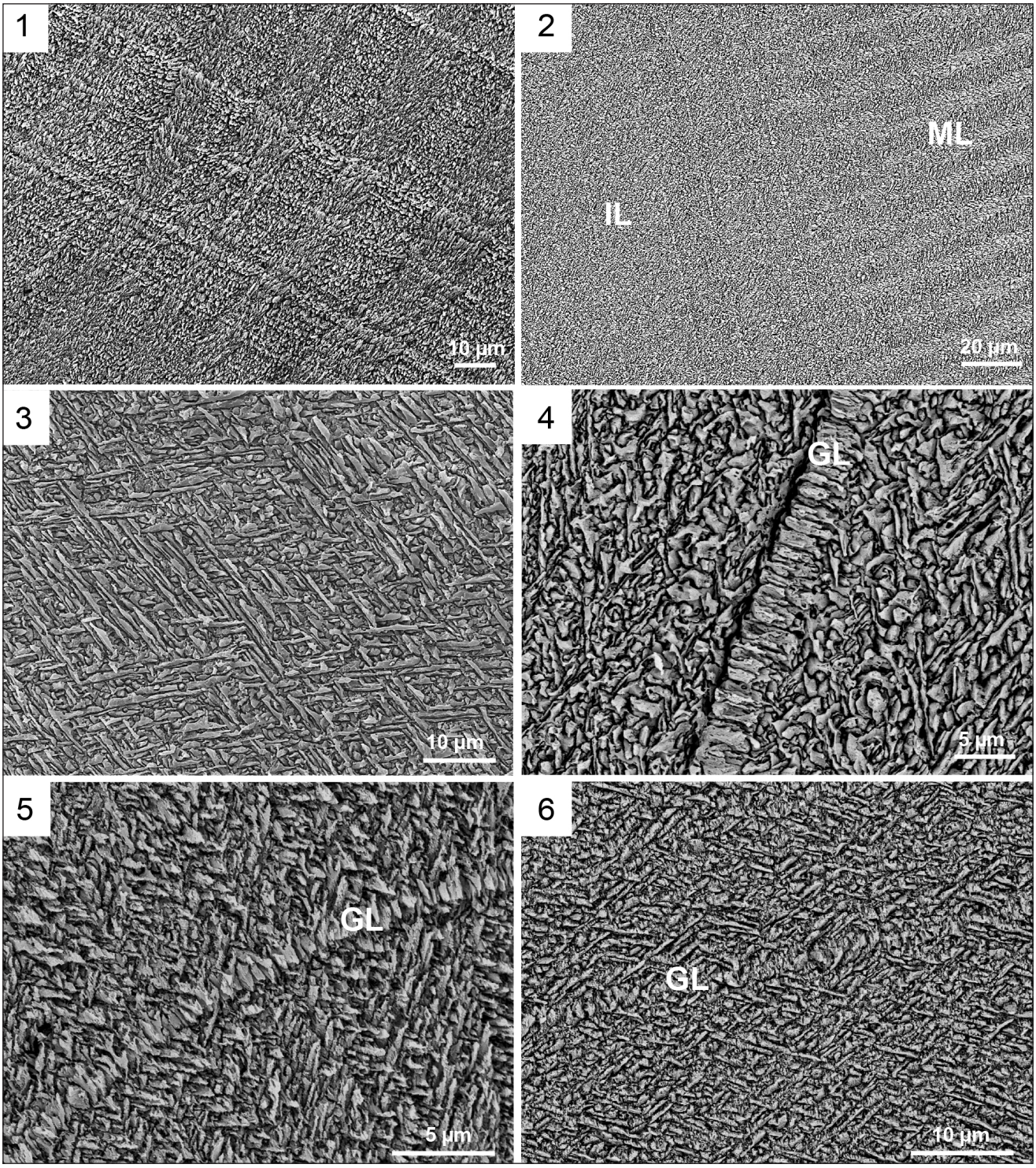

PLATE 4

Scanning Electron Microscope images showing the shell microstructure of specimens of *Tivela stefaninii*. GL: growth lines; IL: inner layer; ML: middle layer.

Fig. 1 - Linear crossed lamellar middle layer crossed by numerous growth lines. Specimen BS-246, right valve.

Fig. 2 - Gradual boundary between the linear crossed lamellar middle layer and the fine complex crossed lamellar inner layer, not defined by a pallial myostracum. Specimen T1, left valve, image in BED-C.

Fig. 3 - Fine complex crossed lamellar microstructure of the inner layer. Specimen T1, left valve, image in BED-C.

Figs 4-6 - Irregular simple prismatic growth line crossing the fine complex crossed lamellar inner layer. Specimen T1, left valve, image in BED-C.

Kamiya 1968; Taylor et al. 1969; Kobayashi 1976b; Waller 1980; Carter et al. 1990), with a particular focus on *A. broughtonii* (Schrenck, 1867) (Kobayashi & Kamiya 1968; Uozumi et al. 1972; Kobayashi 1976a; Popov 1986; Carter et al. 1990; Nishida et al. 2012, 2015, 2018). The only mention of *A. uropigimelana* is by Carter et al. (1990), who simply observed that the third-order lamellae of the crossed lamellar microstructure are blade-like. The shell microstructure of *A. uropigimelana,* here illustrated, conforms to that reported in congeneric species, as all the specimens are composed of an outer simple crossed lamellar layer and an inner complex crossed lamellar layer. Worthy of note is the occurrence, within a predominant crossed lamellar microstructure, of periodic bands of dendritic nondenticular composite prisms in the outer part of the outer layer. Previous studies (Kobayashi & Kamiya 1968; Kobayashi 1976a, b; Carter et al. 1990; Nishida et al. 2012, 2015, 2018) reported the occurrence of these periodic bands in the outer layer of *A. broughtonii* and *A. ninohensis,* documenting cyclic changes in the shell microstructures of the outer layer during the organism's lifetime. These authors, in describing these bands, all referred to a composite prismatic microstructure. In this study, we were able to better define this fabric as dendritic NDCP (Carter & Sato 2020) and we hereinafter refer to this microstructural type.

Ontogenetic changes in bivalve shell microstructures within a single shell layer are not uncommon and have been described in various bivalve taxa (see tab. 1 in Nishida et al. 2012). Nishida et al. (2012, 2015) observed, in modern specimens of *A. broughtonii,* fluctuations in the relative thickness of the two microstructures (CL and dentritic NDCP) in the outer layer, which reflect seasonal changes in water temperatures. The authors, comparing the shell stable isotope composition with the thickness of these microstructures within the outer layer, noted that the relative thickness of the dendritic NDCP microstructure in the outer layer is greater at cooler temperatures, whereas the CL microstructure is relatively thicker at higher temperatures in summer. In most cases major growth breaks were observed at the positive peaks of thickness of the crossed lamellar structure (Nishida et al. 2012). Kobayashi (1976a, b) noticed in *A. broughtonii* and *A. ninohensis* that the CL microstructure is formed during slower shell growth rates, whereas the dendritic NDCP microstructure is formed during faster shell growth rates. Our observations agree with previous findings. In the *A. uropigimelana* specimens here studied, the crossed lamellar microstructure occurs in the inner part of the outer layer. In correspondence of growth increments, the CL microstructure occurs together with dendritic nondenticular composite prisms, whereas in correspondence of the growth lines only the CL microstructure occurs. As growth lines form during time intervals of slow shell growth (Schöne & Surge 2012), it is reasonable to assume that the CL microstructure, occurring in correspondence of growth lines, is formed at slower growth rates, whereas the dendritic NDCP microstructure, occurring in the growth increments, is formed at faster growth rates. Nishida et al. (2018) document that in long-lived specimens of *A. broughtonii* the relative thickness of the dendritic NDCP microstructure tends to decrease as the individuals grow older. Although seasonal water temperature changes are considered to be the primary factor controlling the relative thickness of the two microstructures, also physiological factors related to aging may play an important role. Indeed, the composite prismatic microstructure is more organic rich compared to the crossed lamellar one (Taylor & Layman 1972; Nishida et al. 2015); the production of the organic matrix is more demanding metabolically than the crystallization of calcium carbonate (Palmer

PLATE 5

Scanning Electron Microscope images showing the shell microstructure of specimens of *Oliva bulbosa*. GL: growth lines; IL: inner layer; M1: middle layer 1; M2: middle layer 2; OL: outer layer; OS: outer surface; TL: transitional layer.

Fig. 1 - Shell section showing the five different crossed lamellar layers. Specimen MS-24.

Fig. 2 - A major growth line in the outer layer showing a well-defined irregular simple prismatic microstructure; minor and faint growth lines also occur. Specimen OB1.

Fig. 3 - The transitional layer, crossed by numerous tidally controlled growth lines, separates the branching crossed lamellar outer layer and the linear crossed lamellar middle layer 1. Specimen BS-49.

Fig. 4 - A patch of transitional layer defined by the occurrence of numerous growth lines. Specimen OB1.

Figs 5-6 - Tidally controlled growth lines in the transitional layer. In fig. 5 it shows the branching crossed lamellar microstructure of the outer layer, whereas in fig. 6 its microstructure is not well defined as it is entirely masked by growth lines. Specimen MS-24 (5), specimen OB1 (6).

Fig. 7 - Irregular simple prismatic growth line in the middle layer 2. Specimen MS-24.

Fig. 8 - Sharp boundary between the crossed lamellar middle layer 1 and middle layer 2. Specimen BS-49.

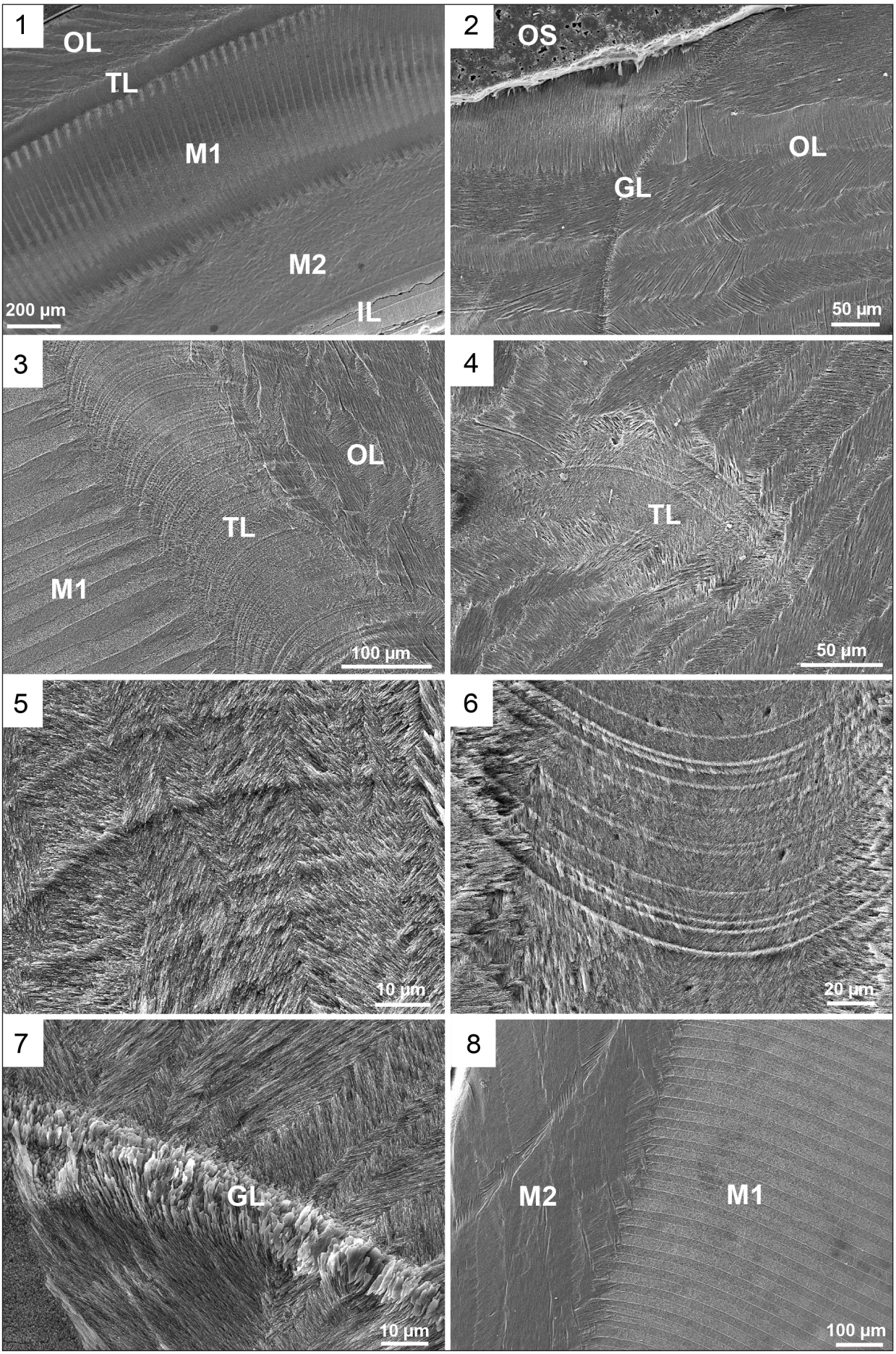
1
OL
TL
M1
M2
IL
200 µm
2
OS
OL
GL
50 µm
3
OL
TL
M1
100 µm
4
TL
50 µm
5
10 µm
6
20 µm
7
GL
10 µm
8
M2
M1
100 µm

PLATE 5

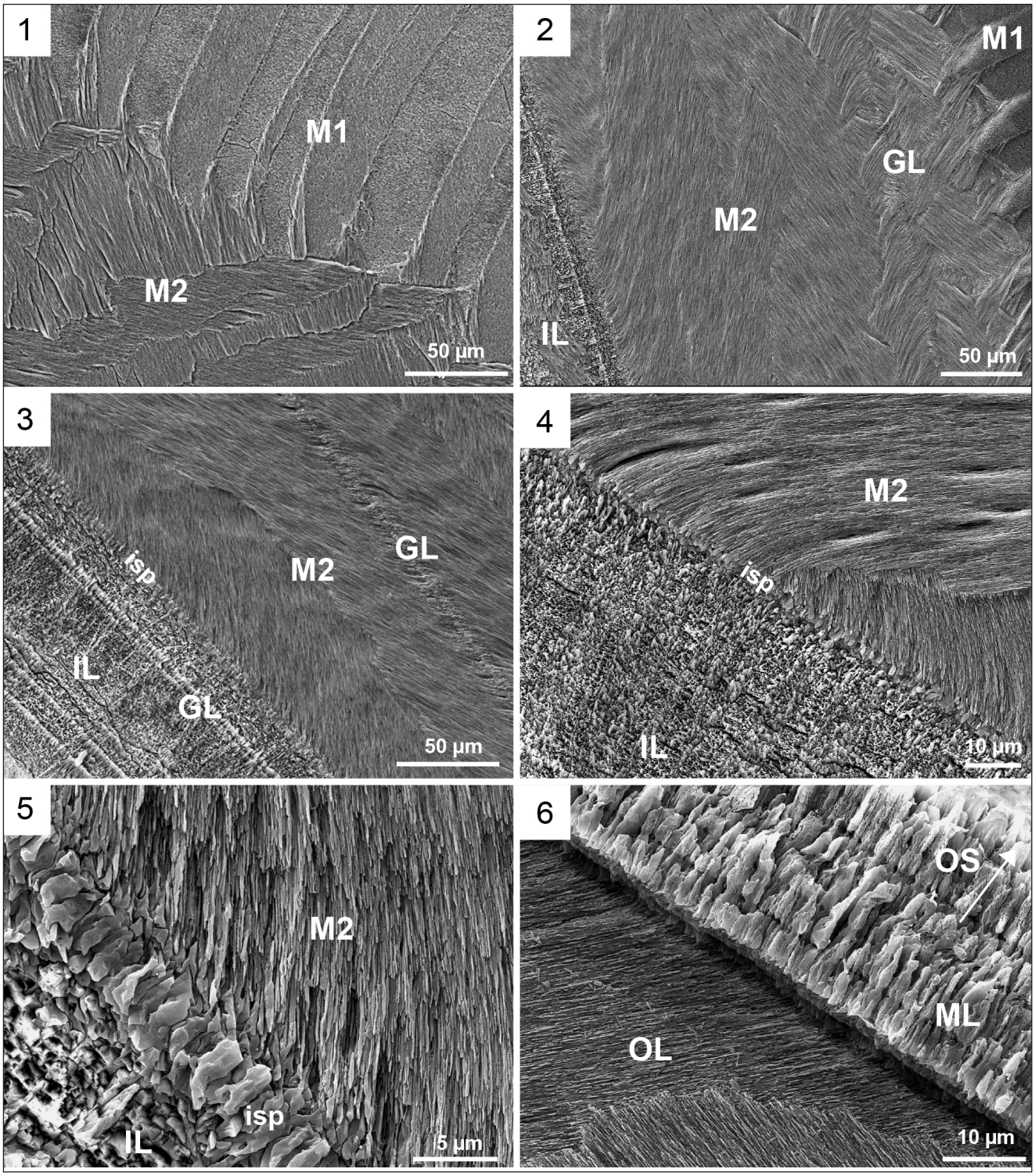

Plate 6

Scanning Electron Microscope (SEM) images showing the shell microstructure of specimens of *Oliva bulbosa*. GL: growth lines; isp: thin layer of irregular simple prisms; IL: inner layer; M1: middle layer 1; M2: middle layer 2; ML: myostracal layer; OL: outer layer; OS: outer surface.

Fig. 1 - Sharp boundary between the crossed lamellar middle layer 1 and middle layer 2. Specimen BS-49.

Fig. 2 - Shell section showing the middle layer 1, the middle layer 2 and the inner layer, all composed of linear crossed lamellae with different orientations with respect to the outer shell surface. The middle layer 2 is crossed by a growth line. Specimen MS-24.

Fig. 3 - Boundary between the crossed lamellar middle layer 2 and the inner layer, separated by an irregular prismatic thin layer. Growth lines crossed both layers. Specimen MS-24.

Figs 4-5 - Sharp boundary between the middle layer 2 and the inner layer defined by a thin layer of irregular simple prisms. Specimen OB1 (4), specimen MS-24 (5).

Fig. 6 - Irregular simple prisms of a myostracal layer in the outer part of the columella representing the attachment site of the columellar muscle. Specimen MS-24.

1983, 1992), thus it is likely that with age the organisms shift to a production of a microstructure with less organic matrix and thus metabolically speaking cheaply, possibly explaining why in the ventral part dendritic NDCP are not common. In our examined specimens, we did not observe a decrease in thickness of the dendritic NDCP bands towards the ventral part, i.e. the senile part of the shell, but more specimens need to be investigated to confirm this finding.

Tivela stefaninii

The shell microstructure of the species *Tivela stefaninii* is composed of three aragonitic layers: an outer composite prismatic, a middle crossed lamellar and an inner fine complex crossed lamellar. Middle and inner layers are not separated by a distinct pallial myostracum. According to Carter & Sato (2020) in a few bivalves, the boundary between middle and inner layers is characterised by a discontinuous pallial myostracum or by its absence, as happened in most oysters. In such cases, the middle/inner layer boundary may be marked by a clear change in shell microstructure. This is not the case of *Tivela stefaninii*, where generally the simple crossed lamellae of the middle layer pass gradually into the fine complex crossed lamellae of the inner layer.

Only the shell microstructure of two species belonging to the genus *Tivela* was briefly described and illustrated in previous studies: *Tivela trigonella* (Lamarck, 1818), which according to Carter (1990) has a fibrous prismatic outer layer, a simple crossed lamellar middle layer and an inner layer composed of acicular crossed lamellae to fine complex crossed lamellae, and *Tivela byronensis* (Gray, 1838) whose inner layer with a fine complex crossed lamellar microstructure is figured by Carter et al. (2012) and Carter & Sato (2020). *Tivela stefaninii* show the same three-layer organisation of the congeneric species, but the outer layer is composite prismatic, possibly with a spherulitic origin, and not fibrous prismatic as in *T. trigonella*. Indeed, the outer layer in *T. stefaninii* is made of first order prisms composed of second order prisms radiating from a spindle toward the depositional surface, instead of elongated and parallel first order prisms, like in *T. trigonella*. The etching with hydrochloric acid used in the SEM sample preparation highlights a lower order structure in second order fibrous prisms, which seem to be composed of thin prisms radiating in a fan-like way from a central longitudinal axis, similarly to what illustrated by Amano & Hikida (1999, fig. 4a) in the Miocene venerid species *Kaneharaia ausiensis* (Ilyna, 1954). Unfortunately, as Carter (1990) did not figure the fibrous prismatic outer layer of *T. trigonella*, we do not have the possibility to check and compare the microstructure of the outer layer of *T. trigonella* with that of *T. stefaninii*.

Numerous growth lines cross the outer and middle shell layers; they are observable both at the naked eye in section, due to their dark colour compared to the growth increment, and at the SEM images, but it is often difficult to discern between major and minor/disturbance growth lines, the latter reflecting growth interruptions usually induced by storms, predation or extreme and abnormal environmental conditions (Clark 1974). Disturbance growth lines can be distinguished from periodic and more regular growth lines by abrupt changes in microincrement widths (Schöne & Surge 2012; Moss et al. 2021). Furthermore, they are usually less prominent than annual growth lines and do not extend to the entire length of the shell, tending to disappear near the anterior and posterior margins (Richardson 2001). In contrast to *A. uropigimelana,* where major growth lines show a typical irregular simple prismatic microstructure, form a step on the outer shell surface and are continuously traceable within the entire outer shell layer and on the outer shell surface, in *T. stefaninii* these features are not so clear, hence the difficulty in distinguishing between major and minor growth lines.

The genus *Tivela* Link, 1807 belong to the subfamily Meretricinae, family Veneridae. Other two extant genera belong to the same subfamily: *Gomphina* Mörch, 1853 and *Meretrix* Lamarck, 1799. Few studies analysed the shell microstructure of venerid species and its phylogenetic implications, including the Meretricinae, namely Shimamoto (1986) and Hikida (1996). Both studies reported for the Meretricinae middle and inner homogeneous layers; the outer layer is crossed lamellar for Shimamoto (1986) and fine complex crossed lamellar for Hikida (1996). These data are not supported by our analysis. However, in both these studies only species belonging to the genus *Meretrix* were investigated as representatives of the Meretricinae. No data are available on the shell microstructure of *Tivela* and *Gomphina*, as well as, for what we know, no updated and exhaustive data on the venerid microstructure

and its phylogenetic implications exist. According to Mikkelsen et al. (2006) the subfamily Meretricinae needs an in-depth generic revision, as well as broader systematic studies on Veneridae are needed. Indeed, venerid classification has been historically unstable in terms of taxon placement and higher-order arrangement. As the shell microstructure represents an important character in phylogenetic analyses, with our in-depth investigation we provide detailed descriptions and illustrations of the different shell layers of *Tivela stefaninii* that may be of help for a systematic revision of the subfamily.

Oliva bulbosa

The shell microstructure of the species *Oliva bulbosa* is characterised by an alternation of at least four aragonitic layers composed of linear or branching crossed lamellar microstructure, plus a transitional layer whose peculiarity is the occurrence of numerous growth lines. All layers are crossed by growth lines. The middle layer 2 and the inner layer are separated by a thin continuous layer of irregular simple prisms, similar for its microstructure and its position within the shell to the bivalve pallial myostracum. To better understand the nature of this layer, additional analyses on other *O. bulbosa* specimens are needed.

Data on the shell microstructure of several species of the genus *Oliva* are provided by Tursch & Machbaete (1995). Although *O. bulbosa* microstructure was not described by these authors, our results fit well with their general observations on the shell layering of the genus *Oliva*. In our study we illustrate in detail the shell of *O. bulbosa*, defining the crossed lamellar microstructural type in each layer, subdividing the middle layer into two sublayers (middle layer 1 and 2), and characterising the microstructure of the transitional layer (=transition zone for Tursch & Machbaete 1995) and of additional outer layers. Tursch & Machbaete (1995), based on the different orientation of the crossed lamellae within each layer, divided Indo-Pacific species of *Oliva* into two groups represented respectively by *Oliva reticulata* (Röding, 1798) and *Oliva amethystina* (Röding, 1798). The only feature that distinguishes these two groups is the different orientation of crossed lamellae in the outer layer: in the first group the lamellae are oriented perpendicularly to the outer lip as in the inner layer, whereas, in the second group they are directed obliquely to the outer lip. However, the orientation of crossed lamellae in the outer layer cannot be considered a taxonomical character to distinguish *Oliva* species, as variations in the crossed lamellar directions can occur within the outer layer of a single specimen.

Concerning the transitional layer, it was mentioned by Tursch & Machbaete (1995) as a transition zone with an ill-defined crystal structure, but it was not described in detail. The transitional layer in *O. bulbosa* shells occurs between the outer layer and the middle layer 1 and is defined by the presence of numerous growth lines. Schöne et al. (2005) observed the occurrence of this layer in *Oliva spicata* (Röding, 1798), noting that crystal structures of the crossed lamellar layer slightly obliterate the growth patterns. These authors also affirmed that these growth increments and lines are circalunidian. *Oliva bulbosa* shells analysed in this study show major growth lines, crossing both outer and middle layers, most likely annual, and numerous minor growth lines, crossing only the transitional layer. This minor growth lines can be circalunidian, as in *O. spicata*, or tidally controlled. This may be consistent with the life habitat of *O. bulbosa* in Oman, as this species lives in intertidal settings along the coasts of Oman affected by tidal cycles (e.g. Bosch & Bosch 1982; ElMali 1999; Callapez & Dinis 2020). As observed by Schöne & Surge (2012), bivalve shells from intertidal settings exhibit distinct, tidally controlled growth patterns. Shell growth stops when the organism is aerially exposed during low tide (growth line formation) and begins when it is submerged during high tide (growth increment formation) (e.g. Evans 1972; Ohno 1989; Schöne & Surge 2012). An in-depth sclerochronological analysis is necessary to confirm these findings and to investigate why this layer is not continuous, but sometimes occur in patches within the shell.

In the present investigation, other two additional outer layers have been identified for the first time in specimens of species of *Oliva*, both occurring in the outer part of the inner whorls and the columella: a linear crossed lamellar layer separated from the outer layer by a stockade of thin prisms, and an irregular simple prismatic layer seemingly crossed by growth lines. The first represents the callus. Pietsch et al. (2021) observed in *Olivancillaria vesica* (Gmelin, 1791) and *Olivancillaria auricularia* (Lamarck, 1811), both belonging to the family Olividae as *O. bulbosa*, that the callus is composed of

a crossed lamellar microstructure and it is separated from the main shell by a thin prismatic layer, as we observe in our specimens. The second additional layer represents a myostracal layer, i.e. the shell material secreted at sites of shell muscle attachment. According to Carter et al. (2012), these are always aragonitic and almost always show an irregular simple prismatic microstructure. It represents the attachment site of the columellar muscle, the only attachment of the soft parts to the shell (Kantor 1991; Kantor et al. 2017).

Conclusion

In this study we describe for the first time the shell microstructure and mineralogy of three mollusc species, the bivalves *Anadara uropigimelana* and *Tivela stefaninii*, and the gastropod *Oliva bulbosa*, which are abundant in archaeological shell assemblages of the Arabian region and represent powerful tools for high resolution palaeoclimatic and palaeoenvironmental studies (Crippa et al. 2024). The aragonitic specimens analysed at SEM and XRD show an excellent shell preservation, with no trace of diagenetic or anthropic alteration, being thus suitable for geochemical analyses.

In poorly studied or complex groups, like gastropods or Veneridae bivalves, it is important to illustrate and describe the microstructures even of single species as, as observed in previous papers (e.g. Sato et al. 2020) and strengthened by the data presented in this research, there are several differences in the microstructures at family, genus but also at species level.

Anadara uropigimelana shows an aragonitic shell composed of an outer crossed lamellar and an inner complex crossed lamellar layer, separated by an irregular simple prismatic pallial myostracum, and by dendritic nondenticular composite prismatic periodic bands in the outer part of the outer layer. All the shell is crossed by growth lines and tubules. The co-occurrence of dendritic NDCP and crossed lamellae in the outer layer document cyclic changes in the microstructure during the life cycle, which may reflect seasonal changes in water temperatures and differences in the shell growth rate. *Tivela stefaninii* has an aragonitic shell with an outer composite prismatic layer, a middle crossed lamellar layer and an inner complex crossed lamellar layer, whereas *Oliva bulbosa* shell shows an alternation of at least four aragonitic layers composed of linear or branching crossed lamellar microstructure, plus a transitional layer whose peculiarity is the occurrence of numerous tidally controlled growth lines, a crossed lamellar callus and a myostracal layer, representing the attachment site of the columellar muscle.With this analysis, besides providing novel data on the shell fabric of these poorly known mollusc species and having shown their exquisite preservation, we want to emphasize the great potential of investigating shell microstructure and mineralogy, in order to contribute to the advancement of knowledge in mollusc phylogenetics, biology, crystallography and palaeoecology.

Data Availability Statement

The data supporting the results of this research are available upon request. Interested researchers may contact the corresponding Author to obtain access.

Acknowledgements: S. Lischi and M. Cremaschi are acknowledged for providing the specimens here analysed. S. Crespi is warmly thanked for the help in the SEM images acquisition. Two anonymous reviewers are warmly thanked for their comments, which improved the quality of the paper.

References

Amano K. & Hikida Y. (1999) - Evolutionary history of the Cenozoic bivalve genus *Kaneharaia* (Veneridae). *Paleontological Research*, 3(4): 249-258.

Bieler R., Mikkelsen P.M., Collins T.M., Glover E.A., González V.L., Graf D.L., Harper E.M., Healy J., Kawauchi G. Y., Sharma P.P., Staubach S., Strong E.E., Taylor J.D., Tëmkin I., Zardus J.D., Clark S., Guzmán A., McIntyre E., Sharp P. & Giribet G. (2014) - Investigating the Bivalve Tree of Life - an exemplar-based approach combining molecular and novel morphological characters. *Invertebrate Systematics*, 28(1): 32-115.

Bøggild O.B. (1930) - The shell structure of the Mollusks. Det Kongelige Danske Videnskabernes Selskabs Skrifter naturevidenskabelig og mathematisk, 231-326.

Bosch D. & Bosch E. (1982) - Seashells of Oman. Addison-Wesley Longman Ltd, 212 pp.

Callapez P.M. & Dinis P.A. (2020) - Mollusc remains from the Quelba/Kalba fortification (late 16th to 18th centuries, Sharjah, UAE): taxonomical, taphonomical, environmental and cultural implications. *Annual Sharjah Archaeology*, 17: 175-216.

Carter J.G. (1980) - Environmental and biological controls of bivalve shell mineralogy and microstructure. In: Rhoads D.C., Lutz R.A. (Eds.) - Skeletal Growth of Aquatic Organisms: Biological Records of Environmental Change (Topics in Geobiology): 69-113. Plenum Publishing Corp, New York.

Carter J.G. (1990) - Skeletal biomineralization: patterns, processes and evolutionary trends. Short courses in geology.

Van Nostrand Reinhold, New York, 5, 832 pp.
Carter J.G. & Sato K. (2020) – Bivalve shell microstructure and mineralogy: Shell microstructure terminology. Part N, Revised, Volume 1, Chapter 2A. Treatise Online, 137, 81 pp.
Carter J.G., Harries P.J., Malchus N., Sartori A.F., Anderson L.C., Bieler R., Bogan A.E., Coan E.V., Cope J.C.W., Cragg S.M., García-March J.R., Hylleberg J., Kelley P., Kleemann K., Kříž J., McRoberts C., Mikkelsen P.M., Pojeta J. Jr., Skelton P.W., Tëmkin I., Yancey T. & Zieritz A. (2012) - Illustrated Glossary of the Bivalvia. Part N, Revised, Volume 1, Chapter 31. Treatise Online, 48, 209 pp.
Casella L.A., Griesshaber E., Yin X., Ziegler A., Mavromatis V., Müller D., Ritter A.-C., Hippler D., Harper E.M., Dietzel M., Immenhauser A., Schöne B.R., Angiolini L. & Schmahl W.W. (2017) - Experimental diagenesis: insights into aragonite to calcite transformation of *Arctica islandica* shells by hydrothermal treatment. *Biogeosciences,* 14: 1461-1492.
Checa A. (2018) - Physical and biological determinants of the fabrication of molluscan shell microstructures. *Frontiers in Marine Science*, 5: 353.
Checa A. & Salas C. (2017) - Periostracum and shell formation in the Bivalvia. Part N, Revised, Volume 1, Chapter 3. Treatise Online 93, 53 pp.
Clark G.R. II (1974) - Growth lines in invertebrate skeletons. *Annual Review of Earth and Planetary Sciences* 2: 77-99.
Crippa G., Ye F., Malinverno C. & Rizzi A. (2016) - Which is the best method to prepare invertebrate shells for SEM analysis? Testing different techniques on recent and fossil brachiopods. *Bollettino della Società Paleontologica Italiana,* 55: 111-125.
Crippa G., Lischi S., Chiari A., Dapiaggi M. & Cremaschi M. (2023) - Discovering fire events in the HAS1 settlement on the Dhofar coast (Oman) by a multi-methodological study of mollusk shells. *Quaternary Research*, 113: 105-121.
Crippa G., Lischi S. & Cremaschi M. (2024) - Investigating the Upper Holocene palaeoenvironment and human subsistence strategy in the Khor Rori coastal area by studying mollusc remains from the Inqitat plateau (Dhofar, Sultanate of Oman). *Journal of Quaternary Science*, 39(4): 608-625.
De Paula S.M. & Silveira M. (2009) - Studies on molluscan shells: contributions from microscopic and analytical methods. *Micron,* 40: 669-690.
ElMali A.T. (1999) - Mollusc harvesting along the coasts of Oman: a supplementary diet. *Proceedings of the Seminar for Arabian Studies*, 29: 45-53.
Evans J.W. (1972) - Tidal growth increments in the cockle *Clinocardium nuttalli. Science*, 176: 416-417.
Griesshaber E., Yin X., Ziegler A., Kelm K., Checa A., Eisenhauer A. & Schmahl W.W., (2017) - Patterns of mineral organization in carbonate biological hard materials. In: Heuss-Aßbichler S., Amthauer G. & John M. (Eds.) - Highlights in Applied Mineralogy: 245-272. De Gruyter, Berlin.
Grizzle R.E., Bricelj V.M., AlShihi R.M., Ward K.M. & Anderson D.M. (2018) - Marine molluscs in nearshore habitats of the United Arab Emirates: Decadal changes and species of public health significance. *Journal of Coastal Research*, 34(5): 1157-1175.
Gröcke D.R. & Gillikin D.P. (2008) - Advances in mollusc sclerochronology and sclerochemistry: tools for understanding climate and environment. *Geo-Marine Letters*, 28: 265-268.
Hikida Y. (1996) - Shell structure and its differentiation in the Veneridae (Bivalvia) [in Japanese with English abstract]. *Journal of the Geological Society of Japan*, 102: 847-865.
Jones D.S. (1983) - Sclerochronology: reading the record of the molluscan shell: Annual growth increments in the shells of bivalve molluscs record marine climatic changes and reveal surprising longevity. *American Scientist,* 71: 384-391.
Kantor Y.I. (1991) - On the morphology and relationships of some oliviform gastropods. *Ruthenica*, 1(1-2): 17-52.
Kantor Y.I., Fedosov A.E., Puillandre N., Bonillo C. & Bouchet P. (2017) - Returning to the roots: morphology, molecular phylogeny and classification of the Olivoidea (Gastropoda: Neogastropoda). *Zoological Journal of the Linnean Society*, 180(3): 493-541.
Kennedy W.J., Taylor J.D. & Hall A. (1969) - Environmental and biological controls on bivalve shell mineralogy. *Biological Reviews*, 44: 499-530.
Kobayashi I. (1969) - Internal microstructure of the shell of bivalve molluscs. *American Zoologist*, 9: 663-672.
Kobayashi I. (1976a) - Internal structure of the outer shell layer of *Anadara broughtonii* (Schrenck). *Japan journal malacofauna (Venus),* 35(2): 63-72.
Kobayashi I. (1976b) - The change of internal shell structure of *Anadara ninohensis* (Okuta) during the shell growth. *Journal of the Geological Society of Japan,* 82: 441-447.
Kobayashi I. & Kamiya H. (1968) - Microscopic observations on the shell structure of bivalves - part III genus *Anadara. Journal of the Geological Society of Japan*, 74: 351-362.
Lindauer S., Santos G.M., Steinhof A., Yousif E., Phillips C., Jasim S.A., Uerpmann H.P. & Hinderer M. (2017) - The local marine reservoir effect at Kalba (UAE) between the Neolithic and Bronze Age: an indicator of sea level and climate changes. *Quaternary Geochronology,* 42: 105-116.
Lindauer S., Milano S., Steinhof A. & Hinderer M. (2018) - Heating mollusc shells - A radiocarbon and microstructure perspective from archaeological shells recovered from Kalba, Sharjah Emirate, UAE. *Journal of Archaeological Science*, 21: 528-537.
Lischi S. (2018) - Macroscopic analysis of the bead assemblage from the South Arabian port of Sumhuram, Oman (seasons 2000–2013). *Arabian Archaeology and Epigraphy,* 29: 65-92.
Lischi S. (2019) – Risultati preliminari delle ricerche archeologiche presso l'insediamento HAS1 di Inqitat, Dhofar (2016–2019). *Egitto e Vicino Oriente*, 42: 119-134.
Lischi S. (2022) – Settlement dynamics and territorial organisation in Dhofar between the bronze age and late antiquity: understanding the settlement process of the Khor Rori area and development of a new regional cultural model. Unpublished PhD thesis, University of Pisa, 2 Volumes, 615 pp.
Lischi S. (2023) - A First Definition of the Dhofar Coastal Culture Archaeological Exploration on the Inqitat Promontory in the Khor Rori Area (Dhofar, Sultanate of Oman). Institute for the Study of Ancient Civilizations and Cultural Resources, Kanazawa University. *Ancient Civilizations and Cultural Resources*, 1: 23-38.
Lutaenko K.A. (2011) - Status of the knowledge of the Indo-Pacific Anadarinae (Mollusca: Bivalvia). In: Lutaenko K.

A. (Ed.) - Proceedings of the workshop, Coastal marine biodiversity and bioresources of Vietnam and adjacent areas to the South China Sea, Nha Trang, Vietnam, pp. 95–101. Vladivostok-Nha Trang: Dalnauka.

MacClintock C. (1967) - Shell structure of patelloid and bellerophontoid gastropods (Mollusca). *Peabody Museum of Natural History Yale University, Bulletin*, 22: 1-140.

Martin C. (2005) - Les malacofaunes marines archéologiques du Ja'alan (Sultanat d'Oman): un 680 indicateur des modes de vie des populations dans leur environnement, du Néolithique à l'Âge du Bronze. Unpublished PhD thesis, Muséum National d'Histoire Naturelle, 411 pp.

Meyers M.A., Chen P.Y., Lin A.Y.M. & Seki Y. (2008) - Biological materials: structure and mechanical properties. *Progress in Material Science,* 53: 1-206.

Mikkelsen P.M., Bieler R., Kappner I. & Rawlings T.A. (2006) - Phylogeny of Veneroidea (Mollusca: Bivalvia) based on morphology and molecules. *Zoological Journal of the Linnean Society*, 148(3): 439-521.

Milano S., Prendergast A.L. & Schöne B.R. (2016) - Effects of cooking on mollusk shell structure and chemistry: Implications for archaeology and paleoenvironmental reconstruction. *Journal of Archaeological Science*, 7: 14-23.

Moss D.K., Ivany L.C. & Jones D.S. (2021) - Fossil bivalves and the sclerochronological reawakening. *Paleobiology*, 47(4): 551-573.

Nishida K., Nakashima R., Majima R. & Hikida Y. (2011) - Ontogenetic changes in shell microstructures in the cold seep-associated bivalve, *Conchocele bisecta* (Bivalvia: Thyasiridae). *Paleontological Research*, 15: 193-212.

Nishida K., Ishimura T., Suzuki A. & Sasaki T. (2012) - Seasonal changes in the shell microstructure of the bloody clam, *Scapharca broughtonii* (Mollusca: Bivalvia: Arcidae), *Palaeogeography Palaeoclimatology Palaeoecology*, 363-364: 99-108.

Nishida K., Suzuki A., Isono R., Hayashi M., Watanabe Y., Yamamoto Y., Irie T., Nojiri Y., Mori C., Sato M., Sato K. & Sasaki T. (2015) - Thermal dependency of shell growth, microstructure, and stable isotopes in laboratory-reared *Scapharca broughtonii* (Mollusca: Bivalvia). *Geochemistry, Geophysics, Geosystems*, 16(7): 2395-2408.

Nishida K., Hayashi M., Yamamoto Y., Irie T., Watanabe Y., Kishida C., Nojiri Y., Sato M., Ishimura T. & Suzuki A. (2018) - Effects of elevated CO_2 on shell ^{13}C and ^{18}O content and growth rates in the clam *Scapharca broughtonii*. *Geochimica et Cosmochimica Acta*, 235: 246-261.

Ohno T. (1989) - Palaeotidal characteristics determined by microgrowth patterns in bivalves. *Palaeontology*, 32: 237-263.

Oschmann W. (2009) - Sclerochronology: editorial. *International Journal of Earth Sciences,* 98: 1-2.

Palmer A.R. (1983) - Relative cost of producing skeletal organic matrix versus calcification: evidence from marine gastropods. *Marine Biology*, 75: 287-292.

Palmer A.R. (1992) - Calcification in marine molluscs: How costly is it? *Proceedings of the National Academy of Sciences,* 89: 1379-1382.

Pietsch C., Anderson B.M., Maistros L.M., Padalino E.C. & Allmon W.D. (2021) - Convergence, parallelism, and function of extreme parietal callus in diverse groups of Cenozoic Gastropoda. *Paleobiology*, 47(2): 337-362.

Popov S.V. (1986) - Composite prismatic structure in bivalve shell. *Acta Palaeontologica Polonica,* 31: 1-2.

Posenato R., Crippa G., de Winter N.J., Frijia G. & Kaskes P. (2022) - Microstructures and sclerochronology of exquisitely preserved Lower Jurassic lithiotid bivalves: paleobiological and paleoclimatic significance. *Palaeogeography, Palaeoclimatology, Palaeoecology*, 602: 111162.

Posenato R. & Crippa G. (2023) - An insight into the systematics of Plicatostylidae (Bivalvia), with a description of *Pachygervillia anguillaensis* n. gen. n. sp. from the *Lithiotis* facies (lower Jurassic) of Italy. *Rivista Italiana di Paleontologia e Stratigrafia*, 129(3): 551-572.

Richardson C.A. (2001) - Molluscs as archives of environmental change. In: Gibson R.N., Barnes M. & Atkinson R.J. A. (Eds) - Oceanography and Marine Biology, an annual review 39: 103-164. Taylor and Francis, New York.

Roselló-Izquierdo E., Morales-Muñiz A. & Popov S.V. (2005) - Gihayu: a Late Stone Age fishing station in the coast of Yemen. *Paléorient*, 116-125.

Sato K. & Sasaki T. (2015) - Shell Microstructure of Protobranchia (Mollusca: Bivalvia): Diversity, New Microstructures and Systematic Implications. *Malacologia*, 59: 45-103.

Sato K., Kano Y., Setiamarga D.H.E., Watanabe H.K. & Sasaki T. (2020) - Molecular phylogeny of protobranch bivalves and systematic implications of their shell microstructure. *Zoologica Scripta*, 49(4): 458-472.

Schöne B.R. & Surge D. (2012) - Bivalve Sclerochronology and Geochemistry. Part N, Revised, Volume 1, Chapter 14. Treatise Online, 46, 24 pp.

Schöne B.R. & Gillikin D.P. (2013) - Unraveling environmental histories from skeletal diaries - Advances in sclerochronology. *Palaeogeography, Palaeoclimatology, Palaeoecology,* 373: 1-5.

Schöne B.R., Dunca E., Fiebig J. & Pfeiffer M. (2005) - Mutvei's solution: an ideal agent for resolving microgrowth structures of biogenic carbonates. *Palaeogeography, Palaeoclimatology, Palaeoecology*, 228(1-2), 149-166.

Shimamoto M. (1986) - Shell microstructure of the Veneridae (Bivalvia) and its phylogenetic implications. *Science Reports of the Tohoku University, Second Series (Geology)*, 56(1): 1-39.

Taylor J.D. (1973) - The structural evolution of bivalve shell. *Palaeontology,* 16: 519-534.

Taylor J.D. & Layman M. (1972) - The mechanical properties of bivalve (Mollusca) shell structures. *Palaeontology,* 15: 73-87.

Taylor J.D., Kennedy W.J. & Hall A. (1969) - The shell structure and mineralogy of the Bivalvia. Introduction. Nuculacea - Trigonacea. *Bulletin of the British Museum (National History), Zoology*, 3: 73-77.

Tursch B. & Germain L. (1985) - Studies on Olividae. I. A morphometric approach to the *Oliva* problem. *Indo-Malayan Zoology*, 2: 331-352.

Tursch B. & Machbaete Y. (1995) - The microstructure of the shell in the genus *Oliva*. *APEX 10* (2/3): 61-78.

Uozumi S., Iwata K. & Togo Y. (1972) - The ultrastructure of the mineral in and the construction of the crossed-lamellar layer in molluscan shell. *Journal of the Faculty of Science, Hokkaido University. Series 4, Geology and mineralogy*, 15(3-4): 447-477.

Yamaguchi K., Seto K., Takayasu K. & Aizaki M. (2006) - Shell layers and structures in the brackish water bivalve, *Corbicula japonica*. *The Quaternary Research (Daiyonki-Kenkyu),* 45(5): 317-331.

Waller T.R. (1980) – Scanning Electron Microscopy of shell and mantle in the order Arcoida (Mollusca: Bivalvia). *Smithsonian contributions to zoology*, 313: 1-58.